Soft Matter

RSC Publishing

PAPER

View Article Online
View Journal | View Issue

Anomalous chain diffusion in unentangled model polymer nanocomposites

Cite this: *Soft Matter*, 2013, **9**, 4336

Gerald J. Schneider,*[a] Klaus Nusser,[b] Susanne Neueder,[b] Martin Brodeck,[b] Lutz Willner,[b] Bela Farago,[c] Olaf Holderer,[a] Wim J. Briels[d] and Dieter Richter[ab]

We studied unentangled poly(ethylene-*alt*-propylene) (PEP) in a composite with hydrophobic silica particles as a function of the filler concentration. Our neutron spin echo (NSE) experiments cover both the internal dynamics as well as the center of mass diffusion beyond the Rouse time. The key experimental results are (i) all of the chains are equally mobile, (ii) the basic segmental (Rouse) relaxation rate is unaffected even at highest filler concentrations, and (iii) apparently the obstacles reduce significantly the translational center of mass motion. This happens, even in the case when the particles do not significantly confine the polymer. (iv) A transition from regular to anomalous diffusion in the Rouse regime at the highest particle fractions is clearly evidenced. In order to understand the microscopic mechanisms underlying the experimental observations, we performed coarse grained simulations. We demonstrate that the geometrical confinement only affects the dynamics at a long time scale outside the experimental window and therefore it is not able to explain the results found in the NSE experiments. The consideration of inter-chain interactions, however, results in a significant influence even at shorter times and a quantitative agreement between the experiments and simulations was found. The simulations clearly demonstrate that the interfaces cause a deceleration of the chains in their close vicinity. Then the inter-chain interactions carry this slowing down to the other chains at a time-scale of the Rouse relaxation time. Hence, in the experimental datasets an overall slowing down is observed.

Received 17th December 2012
Accepted 20th February 2013

DOI: 10.1039/c3sm27886g

www.rsc.org/softmatter

I Introduction

Combining soft polymer matrices with nanoparticles that have high specific surface areas, hybrid materials accounting for a broad range of applications are obtained. The mechanical properties of these nanocomposites are to a large extent determined by the polymer dynamics. However, widely different and even contradictory results are reported. For example, both experiments and simulations aiming at the small scale local dynamics have been reported that point to mobility gradients in the region close to particles.[1–3] These results are reflected by the observation of gradients for the glass transition temperature appearing in the vicinity of surfaces.[2,4] On the other hand, also negligible effects by surfaces are reported.[5,6]

Concerning the intermediate scale, where Rouse dynamics takes place, most of our knowledge is based on simulations that appear to show rather generally an overall slowing down of the Rouse modes[7–9] although some simulations point at a preferential slowing down of the longest wavelength modes[10] only. An interesting review of simulations of polymers in confinement was written by Milchev.[11] A very recent experimental study hints at a slowing down of the Rouse spectrum[12] as well, but a final conclusion cannot be drawn, mostly because adsorption of the chains overshadows confinement effects. Because of such multiple effects it seems to be very difficult to confirm experimentally the anomalous diffusion phenomena predicted by numerical simulations.[13,14]

In order to largely avoid complications due to the adsorption of chains, in the present work we study the single chain polymer dynamics in a nanocomposite with essentially repulsive interactions in the Rouse and diffusion regime. By neutron spin echo (NSE) experiments the single chain dynamic structure factor of the polymer chain in the presence of nanoparticles was directly observed. Surprisingly the internal Rouse relaxation is not affected, even at the highest silica concentrations. On the other hand, the center of mass (c.m.) diffusion is severely modified, signifying itself in a strongly reduced diffusion and a non-Gaussian behavior.

Finally, we performed some simple simulations to be compared with our experimental results. Since we want to address the influence of a broad range of simultaneous confinement lengths on the diffusion of the polymers, we are limited to simulation models which treat each chain as a single

[a]*Jülich Centre for Neutron Science JCNS, Outstation at FRM2, Forschungszentrum Jülich GmbH, 85747 Garching, Germany. E-mail: g.j.schneider@fz-juelich.de*
[b]*Jülich Centre for Neutron Science JCNS 1 and Institute for Complex Systems ICS, Forschungszentrum Jülich GmbH, 52425 Jülich, Germany*
[c]*Institut Laue-Langevin, 6 rue Jules Horowitz, 38000 Grenoble, France*
[d]*Computational Biophysics, University of Twente, 7500 AE Enschede, The Netherlands*

particle. As a result we do not address segmental motions with these simulations.

II Theory

A Rouse dynamics + dynamic structure factors

On intermediate length scales, the microscopic dynamics of a polymer chain in the melt can be described in terms of the Rouse model.[15] This model treats the dynamics of a Gaussian chain in a heat bath. Only entropic forces originating from the conformational chain entropy and frictional forces from the heat bath drive the dynamics. The coherent dynamical structure factor (pair correlation function) reads[15]

$$S(Q,t) = \frac{1}{N_K}\exp\left(-Q^2 D_R t\right)\sum_{m,n}\exp\left[-\frac{Q^2}{6}|m-n|\ell^2 - \frac{2R_{ee}{}^2Q^2}{3\pi^2}\times\sum_{p=1}^{N}\frac{1}{p^2}\left\{\cos\left(\frac{p\pi n}{N}\right)\cos\left(\frac{p\pi m}{N}\right)\times\left[1-\exp\left(-\frac{p^2 t}{\tau_R}\right)\right]\right\}\right] =: S_{c.m.}S_{seg} \quad (1)$$

Its individual parts can be decomposed in three contributions: (i) the first factor describes the contribution of the translational center of mass diffusion, with the diffusion coefficient $D_R = k_B T/(\zeta N) = W\ell^4/(3R_{ee}{}^2)$. Here $W = 3k_B T/(\ell^2\zeta)$ denotes the elementary Rouse rate, ζ refers to the segmental friction and ℓ to the Kuhn length. R_{ee} is the chain end to end distance. (ii) The second factor relates to the static Gaussian structure of the chain. (iii) The third factor containing the sum over the Rouse modes p represents the decay due to the internal dynamics of the coarse grained Rouse chain, characterized by the Rouse time $\tau_R = (\zeta\ell^2N^2)/(3\pi^2k_BT) = N^2/(W\pi^2)$. It is clear from the expressions given that the elementary Rouse rate is the single dynamic parameter of the Rouse model from which all other characteristic values can be deduced.

The corresponding incoherent intermediate scattering function (self-correlation function) is given by

$$S_{inc}(Q,t) = \frac{1}{N_K}\exp\left[-Q^2 D_R t\right]\times\sum_n\exp\left\{-\frac{2R_{ee}{}^2Q^2}{3\pi^2}\sum_{p=1}^{N_K}\frac{1}{p^2}\times\left\{\cos\left(\frac{p\pi n}{N_K}\right)\left(1-\exp\left(-\frac{p^2 t}{\tau_R}\right)\right)\right\}\right\} =: S_{c.m.}S_{seg,inc} \quad (2)$$

In general the total intermediate scattering function is the sum of the S and S_{inc}. For the particular case of a neutron spin echo (NSE) experiment, it is obtained[15,16] as:

$$S_{exp}(Q,t) = \frac{I_{coh}(Q)S(Q,t) - \frac{1}{3}I_{inc}(Q)S_{inc}(Q,t)}{I_{coh}(Q) - \frac{1}{3}I_{inc}(Q)} =: S_{c.m.}S_{seg} \quad (3)$$

The weighting factors $I_{coh}(Q)$ and $I_{inc}(Q)$ denote the Q-dependent coherent and the incoherent scattering intensity. The prefactor of $-1/3$ is caused by the neutron spin flips in incoherent scattering events that change the sign of the recorded amplitude and lowers its magnitude by 1/3.[16]

B Simulations

As already mentioned, our experimental results indicate that only the chain diffusion is substantially affected by the particle addition, while the internal Rouse modes are basically unaffected. In order to understand the reduced diffusion coefficient of the chains we tried two different approaches to simulate the system. In both cases we concentrated on the diffusion of the polymers without any intention to address the faster internal modes or dynamics on the local scale, such as vibrations, CH_3-rotations, *etc.*

In both models used by us polymers are represented as single particles. In order that these particles behave like polymers, in the RaPiD model they will be dressed with additional properties (see below). In contrast, in a model representing each polymer as a chain of connected beads the influence of the small scale dynamics on the slow diffusion of the chain would come out automatically. For the purposes of the present paper, however, such simulations are prohibitively time consuming.

Let us mention at this point that with different aims and at the cost of extremely much computer times simulations of chains in nanocomposites may be feasible. Two such very interesting studies have recently been published. In the paper by Li *et al.*[17] the influence of confinement on tube-diameters has been investigated and reptation times are estimated by extrapolation techniques pioneered by one of the present authors.[18] Kalathi *et al.*[19] performed non-equilibrium simulations of polymer nanocomposites in order to calculate viscosities.

Asakura–Oosawa model. Several simulation studies have been published addressing the diffusion of tracer particles through various confining geometries.[20–22] In all these studies forces between the particles derived from simple spherical potentials. Since it is our intention to obtain some information about the diffusion of tracer particles in the particular confining geometries of our experiments, we decided to achieve this by means of simulations using the simplest model possible, the Asakura–Oosawa model.[23] In this simple model, the tracer particle represents a polymer chain and its position corresponds to the center of mass of the chain. No interactions between the polymers and hard sphere interactions between polymers and colloids were assumed. The colloids were considered to be stationary.

We generated a cubic simulation box containing approx. 1000 spheres while using periodic boundary conditions. The sphere diameters were modeled to obey the same log-normal distribution as the silica particles. The latter was determined by separate experiments,[24] hence there are no unknown parameters. After a random positioning of the spheres in the simulation box, additionally random displacements were performed in order to assure a truly random arrangement (Fig. 1).

In the next step a tracer particle with a diameter representing the coil size of the polymer was placed into the simulation box at a position not occupied by the colloids. The diffusion of this

particle was implemented by performing random jumps with a constant distance of negligible length in a random direction. If collision occurs with one of the colloids during this step, it is rejected. The size of these displacements was chosen to be sufficiently small to ensure that jumps through non-allowed spaces are avoided. By adjusting the diffusion coefficient of the particle moving in the empty box to the value of the unfilled melt, a connection to the time scale of the experimental system can be established. Hence, all simulation parameters are defined. There are no free parameters in the final simulation of the diffusion of the chains in the nanocomposite. In later simulations the radius of the tracer particle was randomly changed during each step following the statistical variation of the polymer size. It was found that, with the given geometrical setup, the variation of the size of the tracer particle ("soft tracer particle") had no influence on the results.

Responsive Particle Dynamics (RaPiD) single particle model. The results of our first simple simulation attempt together with the experimental data suggested that the interaction between polymers plays a significant role in the reduction of the diffusion coefficient. Therefore, we decided to perform additional simulations using a single particle model,[25] based on the Responsive Particle Dynamics (RaPiD) algorithm for the coarse graining of slow variables in soft matter simulations.[26,27]

The RaPiD model applied here includes two ingredients. First, the potential of mean force is represented according to an idea of Pagonabarraga and Frenkel,[28] which takes into account (special) three-body interactions and guarantees a preset compressibility. Second, the RaPiD model introduces a small set of additional dynamical variables n_{ij}, one for each pair of polymers within a prescribed distance of 2.5 times the radius of gyration of the polymers, representing the internal state of the coarse grained polymers. The n_{ij} will be called overlap parameters and have values $n_0(R_{ij})$ at equilibrium. Deviations of the instantaneous values of the n_{ij} from their equilibrium values are used to calculate correction terms to the average forces. The instantaneous forces so obtained may deviate substantially from the average forces. From the point of view of dynamic coarse graining the forces on the coarse particles depend on the recent history described by the time evolution of the internal degrees of freedom. The inclusion of such memory effects[27,29] is necessarily of a somewhat *ad hoc* character, based on physical intuition of the investigator, and can only be substantiated by explicit small scale simulations. The usefulness of the model may be illustrated by many successful applications of rheology in a wide range of soft matter systems.[29] In the present application all model parameters will be tuned to describe the neat melt. The results obtained with confined systems are to be considered as predictions.

Details of the simulation model can be found in the Appendix section.

Calculation of neutron scattering data from simulations. In general, procedures to derive experimental quantities such as the mean squared displacements from simulations are well known. Therefore, we just briefly summarize the most important steps. From both the Asakura–Oosawa and the RaPiD models, we obtain the positions $\boldsymbol{r}$ of the center of masses from the coarse grained polymers as a function of the time t. Once knowing them, we can derive the van Hove self-correlation function $G_s(\boldsymbol{r},t)$, or its respective radial self-distribution function $G(r,t)$ for isotropic systems, with $r = |\boldsymbol{r}|$. It represents the probability of finding a coarse grained polymer at a distance between r and $r + \mathrm{d}r$ after the time t relative to its position at $t = 0$. From this quantity one can directly calculate the mean squared displacement of the center of the mass $\langle r^2_{\mathrm{c.m.}}\rangle$ (ref. 15)

$$r^2_{\mathrm{c.m.}} = \int_0^\infty r^2\left(4\pi r^2 G_s(r,t)\right)\mathrm{d}r \tag{4}$$

or the respective higher moments, *e.g.* $\langle r^4_{\mathrm{c.m.}}\rangle$. As reported below, describing the van Hove self-correlation function by a Gaussian function for the center of mass displacements is only a first order approximation. In order to quantify deviations, a second order parameter $\alpha_2(t)$, referred to as non-Gaussianity parameter, can be introduced. Knowing the moments of the center of mass displacements, it can be calculated directly by[15]

$$\alpha_2(t) = \frac{3}{5}\frac{\langle r^4(t)\rangle}{\langle r^2(t)\rangle^2} - 1. \tag{5}$$

In the Gaussian approximation $\alpha_2(t)$ is zero. A more detailed description can be found in the literature, *e.g.* in a recent paper of Brodeck *et al.*[30]

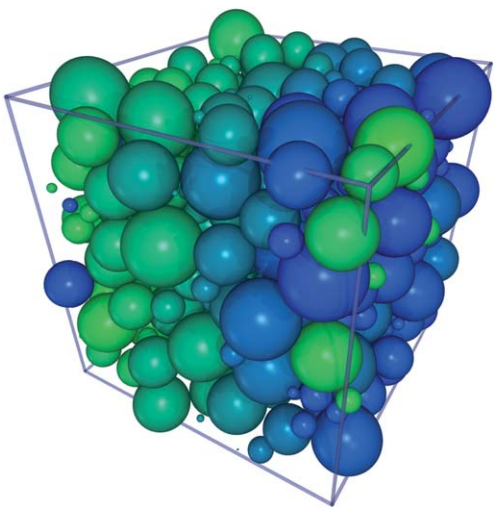

Fig. 1 Image of spheres in the cubic simulation box. The occupied space equals a particle fraction $\Phi = 0.6$. The polydispersity follows the experimentally observed log-normal distribution with a width 0.32.

III Experimental

Samples

The experiments were performed on a model system consisting of hydrogenated 1,4-polyisoprene chains [poly(ethylene-*alt*-propylene) (PEP)] that were anionically synthesized and Nissan ORGANOSILICASOL Tol-St (silica) particles at volume fractions $0 \le \Phi \le 0.6$. Unless stated otherwise, the silica fraction is given in volume percent (vol%). The deuterated and protonated PEP

chains had a molecular weight of 3 kg mol^{-1} with a molecular weight distribution $M_w/M_n \leq 1.03$. The polymer radius of gyration is 1.93 ± 0.03 nm and does not depend on the particle fraction in the given particle range.[24] According to ref. 24 the Nissan particles possess a radius of $R_{av} = (8.5 \pm 0.1)$ nm with a size distribution following a log-normal distribution $1/\sqrt{(2\pi\sigma^2)}$ $\exp(-\ln(R/R_{av})^2/(2\sigma^2))$ with $\sigma = 0.32 \pm 0.02$. The particle surface is coated by short hydrocarbons rendering them hydrophobic. By that means, the system becomes essentially repulsive and should avoid all adhesion effects.

In the first series of small angle neutron scattering (SANS) experiments by contrast variation the scattering length density of the particles was determined to be $\rho_p = 2.95 \times 10^{10}$ cm^{-2}. Because of the hydrophobic coating a core shell structure results that cannot be fully matched. In the Q-range of the dynamic NSE experiments the scattering from the particles was determined earlier and could be corrected for. The best contrast match was achieved for a mixture of H/D PEP of 52/48.[24]

The chain conformation in all samples is that of an ideal random walk, although the $Q^{-1.55}$-dependence at high Q observed in the SANS experiments reveals a finite size effect caused by the low molecular weight. The radius of gyration R_g does not depend on the silica addition, *i.e.* $R_g(\Phi \geq 0) = R_g(\Phi = 0)$.[24]

Neutron spin echo experiments

The NSE experiments were performed on the IN15 spectrometer at the Institut Laue Langevin in Grenoble, France, and on the J-NSE of the Jülich Centre for Neutron Science at the FRM2 in Garching, Germany. We covered a Q-range of 0.5 nm$^{-1} \leq Q \leq$ 1.15 nm^{-1} at 150 °C for times 100 ps < t < 200 ns using two wavelengths $\lambda = 0.8$ nm and $\lambda = 1.68$ nm on the IN15 and $\lambda =$ 0.8, 1.08, 1.2, and 1.7 nm on the J-NSE.

For each sample, a Q-dependent polarization analysis was performed to determine the relative values I_{coh} and I_{inc} of coherent and incoherent scattering in eqn (4). The results of the analysis are given in Table 1.

IV Results

A Experimental

Studying changes of the polymer dynamics in nanocomposites requires knowledge of the neat PEP melt. Fig. 2(a) shows the intermediate scattering function $S(Q,t)/S(Q)$ of PEP at $T = 150$ °C, for four different Q values. The lines are the best fits by the Rouse model, taking into account the contributions from coherent and incoherent scattering by eqn (3). The values for I_{coh} and I_{inc} are taken from Table 1. The chain end-to-end distance, R_{ee}, and in this way the characteristic ratio C_∞ were

Table 1 Relative contributions I_{inc} and I_{coh} by incoherent and coherent scattering, respectively

Q [nm^{-1}]	I_{inc}	I_{coh}
0.50	0.099	0.901
0.77	0.120	0.880
0.96	0.148	0.852
1.15	0.170	0.830

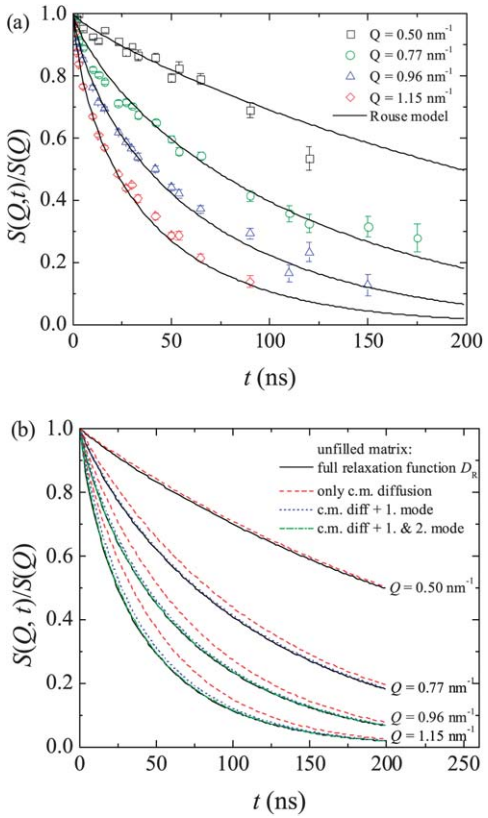

Fig. 2 (a) Dynamic structure factor of bulk PEP (□ Q = 0.5 nm^{-1}, ○ Q = 0.77 nm^{-1}, △ Q = 0.96 nm^{-1} and ◇ Q = 1.15 nm^{-1}). The solid lines represent the prediction by eqn (3). (b) Rouse mode analysis. Contributions by the different modes.

obtained separately by means of small angle neutron scattering experiments.[24] The only remaining free parameter in the fit is the Rouse rate W (or $W\ell^4$; $\ell = \ell_0 C_\infty$; ℓ_0 = bond length) from which the Rouse relaxation time, τ_R, the center of mass diffusion, D_R, and the friction coefficient, ζ, can be deduced as described in the Theory section.

The best description of the experimental datasets was achieved by a joint fit of all Qs with eqn (3) and $W\ell^4 = 0.93 \pm 0.02$ nm^4 ns^{-1}. Within the error bars this value agrees very well with $(W\ell^4)_{lit} = 0.95 \pm 0.07$ nm^4 ns^{-1} at $T = 150$ °C reported in the literature.[31] From our experimentally determined Rouse rate, a Rouse relaxation time $\tau_R = 55 \pm 1$ ns, a center of mass diffusion coefficient $D_R = 1.38 \pm 0.01$ Å^2 ns^{-1} and a friction coefficient $\zeta = 2.1 \pm 0.1 \times 10^{-11}$ N s m^{-1} are calculated.

Before considering the polymer dynamics within the composites, a short look on the individual contributions from the Rouse modes and the center of mass diffusion in eqn (1) and (2) to the full relaxation function of the pure melt is rather helpful. Fig. 2(b) evidences that at $Q = 0.5$ nm^{-1}, basically only the center of mass diffusion (dotted, red line) contributes. Hence, at the corresponding length-scale the c.m. diffusion dominates. However, when comparing the diffusion and the full relaxation function contribution it becomes obvious that with increasing momentum transfer the segmental Rouse relaxation modes start to play a role. Nevertheless, taking into account

only the first two modes, $p = 1$ and $p = 2$, even at the highest $Q = 1.15$ nm^{-1}, the full relaxation function is well described. Thus, we conclude that our experimental data are a result of the motion of the whole chain and the relaxation of the 2 longest wavelength Rouse modes, whereas contributions on a more local scale are not visible.

In the next step we examine the influence of the nanoparticles on $S(Q,t)$ at the intermediate $Q = 0.96$ nm^{-1}. Fig. 3 displays the intermediate scattering functions from the samples with particle fractions between $0 \leq \Phi \leq 0.6$. A pronounced deceleration of the correlation loss with increasing amount of particles is observed, indicating a slow down or confinement of the polymer chain motion. We note that scattering caused by the particle itself additionally contributes. In a previous small angle neutron scattering (SANS) study on the same nanocomposite system, *cf.* ref. 24, this particle contribution that is present for $Q \leq 0.7$ nm^{-1} was measured and therefore could be corrected for. Following the SANS analysis the percentage of scattering caused by particles x_{par} and polymer x_{pol} (ref. 24) is given in Table 2. In order to analyze the NSE data, the particle scattering is assumed to be purely elastic on the investigated time scales. This corresponds to a much slower particle dynamics in comparison with the polymer relaxation and can be included in the modeling by replacing S in eqn (3) by

$$S(Q,t) = x_{par}1 + x_{pol}S_{pol}. \quad (6)$$

This implicitly assumes that the particle scattering is predominantly coherent. Any incoherent scattering contribution from the particles would be strongly localized and cause a negative offset of the spectra (Fig. 3) that is not observed.

Taking into account the particle contribution, the first step of analyzing the NSE data is obtaining the Rouse rate $W(\Phi)$ as a function of the particle fraction. In particular changes in comparison to the pure melt value $W_0 := W(\Phi = 0)$ are of interest.

In the first attempt we tried extracting $W(\Phi)$ by the same procedure as for the pure melt. However, a fit of the data over the whole experimental time range turned out to be impossible,

Table 2 Percentage of total scattering caused by polymers and particles at $Q = 0.50$ nm^{-1}

Φ	x_{par}	x_{pol}
0.06	0.00	1.00
0.35	0.08	0.92
0.50	0.12	0.88
0.60	0.25	0.75

because a reasonable description by eqn (3) with $W(\Phi)$ as the only fit parameter fails to simultaneously describe the data at short and long times at high particle fractions. This implies that the impact of the nanoparticle addition is not merely a homogenous slowdown of the segmental chain dynamics, which could be expressed by one lower, effective Rouse rate $W_{eff}(\Phi)$, as predicted in some simulations of nanocomposites, when attractive polymer particle interactions are present.[9]

As a consequence, the determination of $W(\Phi)$ demands a certain procedure. Therefore, in our second attempt, we obtained the Rouse rate by a joint fit of those data in a limited time range $0 < t \leq t_{max}$. Successive reduction of the maximum time t_{max} limits the size of the window and allows extraction of the true Rouse rate, similar to the case of entangled polymers, where entanglements cause the confinement effects.[15] In the limit $t_{max} \to 0$, the constraints are invisible for the chains and hence the true $W(\Phi)$ is retained. This assumption is equivalent to the well-accepted notion in the reptation model for the description of long chains, where an initial Rouse behavior at short times is superimposed by the topological hindrance of entanglements at longer times.

The Rouse rates for the different particle fractions as a function of t_{max} are depicted in Fig. 4, where eqn (3) was simultaneously fitted to the experimental data for all four Q values in the interval $[0; t_{max}]$. It turns out that for all particle volume fractions $W(\Phi) = W_0$ is found in the limit $t_{max} \to 0$.

Obviously, the chain dynamics at short times is not affected by adding impenetrable space. This result confirms well a very recent observation on nanocomposites with higher molecular weight PEP ($M_w = 50$ kg mol^{-1}) and exactly the same silica.[32] With the result that the relaxation spectra change strongly with

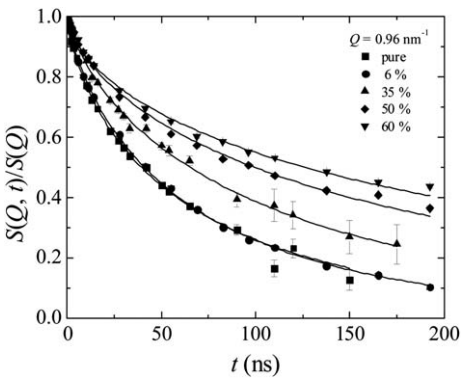

Fig. 3 Dynamic structure factor of PEP at various nanoparticle fractions $0 \leq \Phi \leq 0.6$ at $Q = 0.96$ nm^{-1} (■, ●, ▲, ◆, and ▼ symbols represent $\Phi = 0$, 0.06, 0.35, 0.50 and 0.6, respectively).

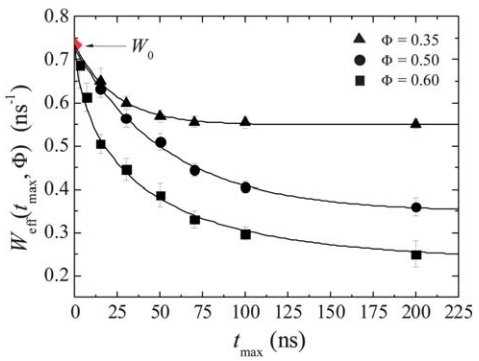

Fig. 4 Dependence of the extracted Rouse rate $W(\Phi)$ on the choice of the fit interval $[0; t_{max}]$ for various particle fractions Φ, *cf.* text.

nanoparticle addition, it becomes evident that the straightforward functional connection between the segmental Rouse rate and the center of mass diffusion, which is valid in the case of unfilled polymer melts, does not exist in nanocomposites.

Knowing that the Rouse rate does not change, it is possible to gain further information on the center of mass diffusion by inspecting the mean squared displacements. For that purpose, we calculate the relaxation function $S_{seg}(Q,t)/S(Q)$ by eqn (4) with $W(\Phi) = W_0$ and $D_R = 0$. Thereby we further assume that the entire internal dynamics is not changed. Given the altogether minute contribution of the internal dynamics to the spectra (see Fig. 4) small changes of the large scale modes would not affect our result much. With this approximation we divide the measured intermediate scattering function by the segmental part and obtain the part only related to the center of mass diffusion, *i.e.* $S_{c.m.} = S_{experimental}/S_{seg}$.

Within the commonly applied Gaussian approximation for diffusive processes we have

$$S_{c.m.} = \exp[-Q^2\langle r^2_{c.m.}(t)\rangle/6], \quad (7)$$

allowing a model independent analysis of the center of mass motion and an interesting test of the Gaussian approximation.

The Gaussianity may be easily tested in comparing data for different Q values. For that purpose, we equate $\langle r^2_{c.m.}(t)\rangle/6 = -\ln(S_{c.m.})/Q^2$. Then, when plotting $\langle r^2_{c.m.}\rangle/6$ as a function of the time in a double logarithmic representation, all curves corresponding to different momentum transfers need to superimpose to one master curve, if the Gaussian assumption is fulfilled.

In this context, first we consider the neat melt (Fig. 5(a)). We note that within the experimental accuracy the data points collapse to one master curve, thus confirming the assumed Gaussian displacement distribution.

A stochastically diffusing object should exhibit a center of mass motion $\langle r^2_{c.m.}(t)\rangle$

$$\ln\left(\frac{\langle r^2_{c.m.}\rangle}{6}\right) = -\ln(D_R) + m\ln(t) \quad (8)$$

with $m = 1$, depicted by the full line in Fig. 5. We want to add that this equation is also fulfilled by a chain in the Rouse model. However, Fig. 5 clearly evidences that the power law for times $t < 55$ ns $= \tau_R$ has a smaller slope, indicating a subdiffusive motion, *i.e.* $m < 1$.

Thus, the experimental data suggest that, in comparison with Brownian diffusion, at early times the increase of $\langle r^2_{c.m.}(t)\rangle$ is reduced compared to the simple Rouse model. Only for diffusion times greater than the decorrelation time $\tau_{deco} \approx \tau_R$ (for short polymers) normal diffusion appears. The slope of about 0.8 ± 0.04 in the double-logarithmic plot at small times shown in Fig. 5(a) confirms well earlier observations by NSE on polybutadiene[33–35] and such on polyethylene,[36] as derived by calculations.[37,38]

Finally, concerning the neat melt, we want to address the diffusion constant D_R, defined in eqn (8) to be the axis intercept. Using Fig. 5(a), the value observed by the intercept is in accordance with $D_R = 1.38 \pm 0.01$ Å^2 ns^{-1} obtained by the description with the Rouse model. Because of our model independent treatment, we know that this value corresponds to the correlation function observed at $t > 55$ ns.

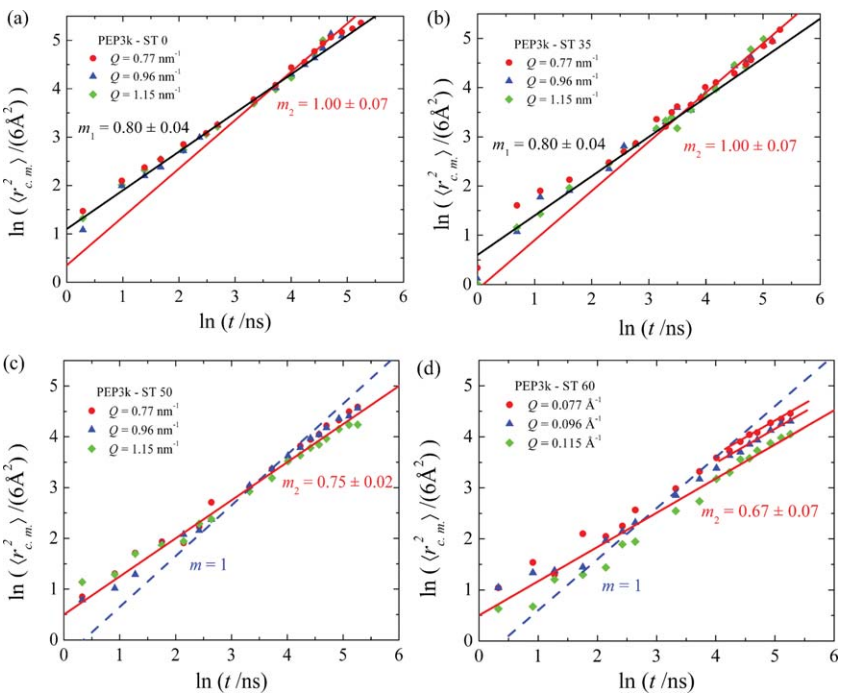

Fig. 5 Natural logarithm of the center of mass mean squared displacement $\langle r^2_{c.m.}\rangle$ *vs.* logarithmic time t. (a) $\Phi = 0$, (b) $\Phi = 0.35$, (c) $\Phi = 0.5$ and (d) $\Phi = 0.6$, in all subfigures, the lines indicate the different power law regions, *cf.* text. Additionally, in panels (c) and (d) the broken line includes $m = 1$ for comparison.

Now, we want to draw our attention to the molecular motion in the nanocomposites. In Fig. 5(b) the datasets from the $\Phi = 0.35$ sample are displayed. Except a change of the axis intercept, corresponding to a reduced polymer diffusion in comparison to the neat melt, there is no obvious change with respect to Fig. 5(a). Even the transition between the two dynamic regimes remains unchanged. Thus, it seems to be very likely that the dynamic regimes (subdiffusive until τ_R and diffusive beyond) are not visibly affected up to $\Phi = 0.35$ though the translational diffusion coefficient is reduced to 0.86 ± 0.01 Å^2 ns^{-1}.

From $\langle r^2_{c.m.}(t)\rangle$ the average distance moved by the center of mass is directly obtained. The overall shift of the $\langle r^2_{c.m.}(t)\rangle$ behavior to lower values evidences that already at very short times the diffusion is reduced. Plotting the average distances at two different times, $t = 150$ ns and $t = \tau_R = 55$ ns (Fig. 6), we observe a decrease as a function of the particle fraction that can be excellently described by a linear function. In a recent work, we calculated the average distance of the polymer center of mass from the closest nanoparticle surface.[32] These values are additionally depicted in Fig. 6. We recognize that the average distance between chains and surfaces is greater than the distance explored by the chains in our experimental time window. In consequence, this indicates that a pure geometrical confinement cannot explain the changes observed. Above, we report anomalous diffusion, even in the pure polymer melt, which is caused by mutual interactions of the polymer chains. Below, using the simplest simulations possible, we want to test, whether such a finite potential between the chains could cause the reduction of the diffusion in our nanocomposites, even though the distance to the impenetrable walls is large.

For the higher particle volume fractions $\Phi = 50\%$ and 60% the short time subdiffusive behavior is retained. However, there is no transition to normal diffusion at long times anymore. The data can still be approximately described by a linear relationship with a slope $m_2 = 0.75 \pm 0.02$ ($\Phi = 0.5$, Fig. 5(c)) and $m_2 = 0.67 \pm 0.07$ ($\Phi = 0.6$, Fig. 5(d)). Thus, anomalous diffusion prevails also for long times.

Also, the datasets in Fig. 5(c) and (d) show that $\langle r^2_{c.m.}(t)\rangle$ taken from spectra at different momentum transfers, using eqn (8), do not superimpose. This indicates that the assumption of a Gaussian displacement distribution is violated. Such a non-Gaussianity might be caused by the heterogeneity involved in a confined motion, similar to chain dynamics in a tube[39] or a diffusion in a polydisperse environment of spherical cavities.[40,41]

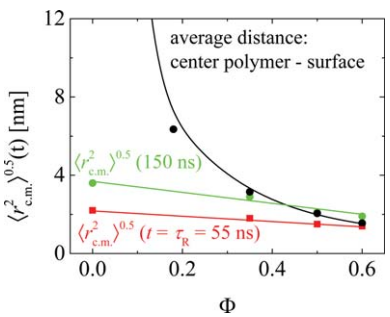

Fig. 6 Comparison of the average distance of the center of mass of the polymers and the surface with mean distances explored by the center of mass $\langle r^2_{c.m.}(t)\rangle^{0.5}$ at the Rouse time $t = \tau_R$ and the maximum time of the experimental window $t = \tau_{max}$ as a function of the particle fraction. The lines serve as a guide to the eye.

In order to quantify the violation of the Gaussian assumption, we use the Rahman, Singwi, Sjölander cumulant expansion[42] in the formulation by Zorn.[43]

$$S_{c.m.} = A_0 \exp\left[- Q^2 \langle r^2(t)\rangle/6 + \frac{\alpha_2(t)}{72} \langle r^2(t)\rangle^2 Q^4 \right]. \quad (9)$$

In comparison to eqn (7), eqn (8) includes the second order expansion in Q^2. It includes the non-Gaussianity parameter $\alpha_2(t)$. A non-vanishing α_2 causes deviations from Gaussian behavior as observed in Fig. 5(c) and (d) at long times. When plotting $\ln(S_{c.m.})$ *vs.* Q^2 the variables $\langle r^2_{c.m.}(t)\rangle$ and α_2 can be in principle directly extracted. However, because of the low number of Q values it is not possible to obtain $\alpha_2(t)$ each time separately. Therefore, we determined $\alpha_2(t)$ by fitting $\ln(S_{c.m.})$ *vs.* Q^2 resulting in a noisy α_2-data. Then in the second step we introduced the averaged α_2-values into eqn (9) and compared with the experimental results. This procedure leads to a good description of $S_{c.m.}(Q,t)$ and shows that the averaged values are a reasonable approximation for $\alpha_2(t)$. Of course, in case there is no splitting visible in Fig. 5, $\alpha = 0$. For $t > 55$ ns, we obtained $\alpha = 0$ (0%), 0.2 ± 0.1 (35%), 0.3 ± 0.1 (50%), and 0.3 ± 0.1 (60%, $t <$ 85 ns) and 0.5 ± 0.1 (60%, $t > 85$ ns).

B Comparison with simulation results

Before presenting the simulation result, we summarize the essential facts. (i) The segmental dynamics of the chains in the nanocomposite is unchanged. (ii) Because of interchain interactions, the neat melt shows anomalous c.m. diffusion. (iii) The translational diffusion is significantly reduced, even at short times. The functional dependency of the related mean squared displacement is unchanged for $\Phi < 0.35$. (iv) At particle fractions $\Phi \geq 0.5$ a loss of the Gaussian behavior is observed and anomalous diffusion occurs over the full range.

Asakura–Oosawa model. Since the segmental dynamics is unchanged, we focus on the deceleration of the center of mass diffusion. With respect to our experimental model system we assumed there are no interactions between different polymers and hard sphere interactions between polymers and colloids according to the Asakura–Oosawa model.[23] More precisely, we consider the simple diffusion of one tracer particle, representing the polymer chain, in a random environment of impenetrable space, imitating the silica particles. The diameter and the polydispersity of the fixed particles correspond to the experimentally determined values. Our first simulation uses a moving tracer particle with a radius $R = R_g = 1.93$ nm. Fig. 7 displays the resulting diffusion coefficients depending on time. The black flat line refers to the situation without colloids. The small variations at higher times correspond to the statistical error of the simulations. Adding impenetrable space to the system leads to a time dependent diffusion coefficient that systematically depends on the free diffusion space left. Three different regions can be identified in the plot. For times $t < 10^2$ ns there are only

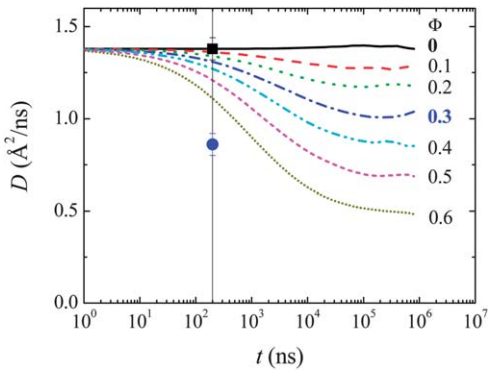

Fig. 7 Calculated diffusion coefficient of a particle moving through an environment of randomly packed colloids with different sphere fractions Φ. For comparison, D_R for $\Phi = 0$, and 0.35 are included. The related $D(t)$ from simulations are highlighted. Within the Rouse model, D_R does not depend on the time. Therefore, we put D_R at a t corresponding to the maximum time available in our NSE window, as indicated by the vertical line.

minor effects, corresponding to chains that are still exploring the local environment. Contact with the colloids is rather seldom. In the intermediate range between 10^2 and 10^4 ns a significant time dependent reduction sets in. For times $t > 10^4$ ns the particle has diffused through large areas of the system (passing several colloids) and the variation becomes weaker. Hence, for the limit $t \rightarrow \infty$ we find the long-time diffusion coefficient D_{geo}.

Within the experimental NSE window ($0.2 < t < 200$ ns), however, no significant reduction of the dynamics of the polymer particles is observed in Fig. 7. Even for $\Phi = 0.6$ the diffusion coefficient only changes by $\approx$15%. Considering the corresponding distance that a polymer particle moves on average within 150 ns, the reason for only marginally affecting the particle diffusion in this time window becomes obvious: The average distance travelled by a polymer particle is smaller than the average distance of the center to the surface (Fig. 6), so no significant influence of the surrounding particles can be expected. The free polymer mostly explores the free space (cavities) between the colloids. The influence of the restricted diffusion space increases only at higher times, when the polymer starts to slip through small spaces and enters different cavities. To exclude the possibility of the tracer particle being trapped in a position where a polymer could diffuse through small cavities by an elongation of the chain we have also performed simulations where the radius of the tracer particle was allowed to change. In this case the radius followed the probability distribution function of the radius of gyration of a polymer. The results did not show any significant difference for the results described above. The reason is that the size of the tracer particle is small relative to the size of the impenetrable colloid particles.

To test whether these contradictions of simulation and experimental results, where a significant effect is already observed at very short times, are due to the artificial choice of the simulated particle size, we also performed simulations with a larger diffusing particle having a diameter equal to the end-to-end distance of the polymer ($R_{ee} = 4.73$ nm). For that situation, a stronger reduction of the diffusion coefficient was observed. In the case of $\Phi = 0.6$ it even dropped close to 0 which means that the particle is stuck within the cavities. The time-scale, however, at which the diffusion starts to decrease, remains almost unchanged. We conclude that pure geometrical hindrance does not describe the experimental observations and additional aspects need to be taken into account.

Responsive Particle Dynamics (RaPiD) single particle model. In our second attempt, an ensemble of particles representing the center-of-mass of a polymer chain is placed into the colloidal environment of 16 nm colloids and interactions between the particles are considered. More precisely, we implemented the RaPiD model as described in the Appendix section.

The previously noted subdiffusive behavior was discussed in terms of inter-chain correlations.[33–35] This approach was later confirmed by systematic NSE experiments for which $S_{c.m.}(Q,t)$ was calculated from a generalized Langevin equation for cooperative dynamics.[36–38] The quantitative agreement with the experimental data suggest that the dynamics of a group of slowly diffusing interacting molecules is correlated by the presence of a finite interpolymer potential that causes the observed anomalous diffusion.[33] With a similar quality, assuming not completely screened hydrodynamic interactions, that are usually neglected in polymer melts, the same effects[44–46] were revealed. Nevertheless, both theoretical approaches hint to a subdiffusive behavior caused by interchain interactions.

The first step of using R_g of the polymer as the tracer particles size was to adjust the free parameters of the RaPiD model until the dynamic behavior of neat PEP was recovered. The simulations were used to calculate the mean squared displacement. Fig. 8(a) compares the calculations and experimental mean squared displacement and demonstrates that this procedure works very well. For the dynamical mechanical modulus G^*, the crossing point of the real G' and the imaginary part G'' was reproduced as well. The parameters that were chosen for the simulation of PEP are given in Table 3.

The value for the strength of transient forces α depends on the particular normalization of the overlap parameter n_0 and can only be discussed in relation to values in similar applications. Comparing with other polymers the present value, $\alpha = 20k_BT$, is in the usual range.[25] The overlap friction similarly depends on the normalization of n_0. With the present normalization it should be close to the experimental Rouse friction, 2.1×10^{-11} N s m^{-1}, which it is. The maximum overlap relaxation time is the overlap relaxation time when the two chains in the relevant pair occupy the same position and is found to be 500 ns. This will apply to only very few overlapping pairs. Assuming that the dominant contribution to the dynamics comes from pairs being separated by a value of R which makes $R^2\exp\{-R/\lambda\}$ maximal, we find that the corresponding overlap relaxation time equals 68 ns, not very different from the Rouse time experimentally determined.

Having determined the input parameters simulating the neat melt, there are no additional parameters used for the simulation of the systems containing the colloid particles. The addition of colloids to the system and the resulting

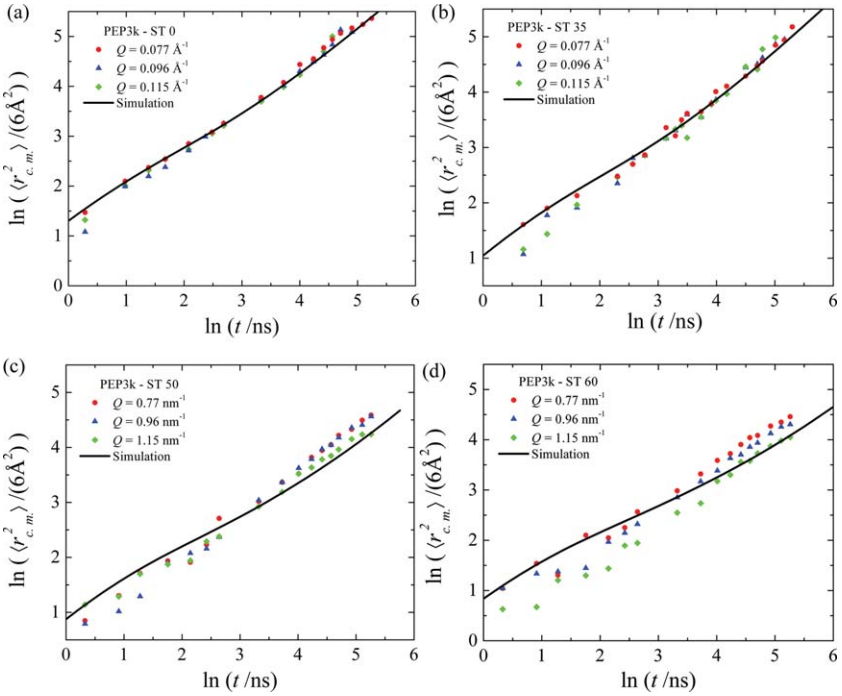

Fig. 8 Comparison of simulated (line) and experimental mean squared displacements. (a) $\Phi = 0$, (b) $\Phi = 0.35$, (c) $\Phi = 0.5$ and (d) $\Phi = 0.6$. In all sub-figures, the lines correspond to the calculation with the RaPiD model, *cf.* text.

Table 3 Parameters for the simulation of the pure PEP melt in the RaPiD model

Strength of transient forces	$\alpha = 20.0 k_B T$
Overlap friction	$\xi_0 = 2.0 \times 10^{-11}$ N s m^{-1}
Maximum overlap relaxation time	$\tau_0 = 5.0 \times 10^{+2}$ ns
Overlap relaxation time decay length	$\lambda = 0.4\ R_g$
Diameter of the colloids	16 nm
Radius of gyration of the polymer	1.93 nm

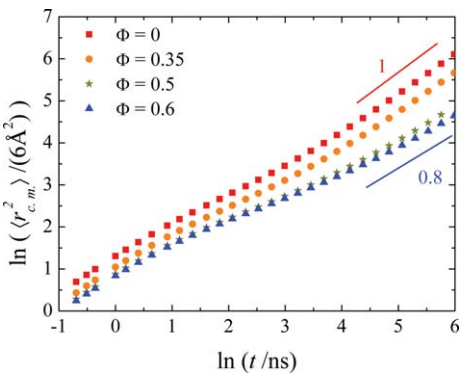

Fig. 9 Comparison of simulated mean squared displacements for various particle fractions Φ. The full lines indicate the slope for normal diffusion ($m = 1$) and subdiffusive behavior ($m = 0.8$).

equilibration of the density were performed in the same way as described in ref. 47. Fig. 8(b)–(d) compare the simulated and the experimental curves of the mean squared displacement. Taking into account that we emphasize on the generic behavior rather than on a detailed agreement, we want to note the excellent agreement even for $\Phi > 0.35$, with respect to retaining the decreasing diffusion and the subdiffusivity of the experiments.

The changes appearing in the center of mass diffusion by adding nanoparticles are visualized in Fig. 9. Obviously $\langle r^2_{\mathrm{c.m.}}(t)\rangle$ is reduced with increasing Φ. In addition, there is a strong change from diffusive behavior (slope = 1) to a subdiffusive behavior (0.8) for $t > t_R = 55$ ns. But, the slopes at short times ($t < t_R$) are more or less the same. A similar behavior was observed in the experiments. But because of knowing all the underlying correlation functions, the simulations allow a more detailed analysis.

The primary quantity describing the diffusion process is the radial van Hove-self-correlation function $G_s(r,t)$ for the coarse grained polymer coils. Fig. 10(a) displays the general behavior: with increasing time the distribution of $\langle r^2_{\mathrm{c.m.}}(t)\rangle$ becomes broader and the height decreases, both for the $\Phi = 0$ and 0.6 samples. To show the effect of nanoparticle addition Fig. 10(b) presents how the distribution changes by adding nanoparticles. Many models, such as the Rouse model, assume a Gaussian distribution for the center of mass displacements. Therefore, comparing the simulated curves with a Gaussian function is rather interesting. We realize clear deviations in the tails of the distribution function for the composite, while the distribution function of the pure polymer melt is well described by a Gaussian distribution function.

The deviations from the Gaussian distribution function can be quantified by including higher order terms in the analysis, in particular the second order non-Gaussian parameter $\alpha_2(t)$, defined by eqn (5). The results for the different particle concentrations are shown in Fig. 11. There a gradual increase from virtually zero at short times to finite values is observed.

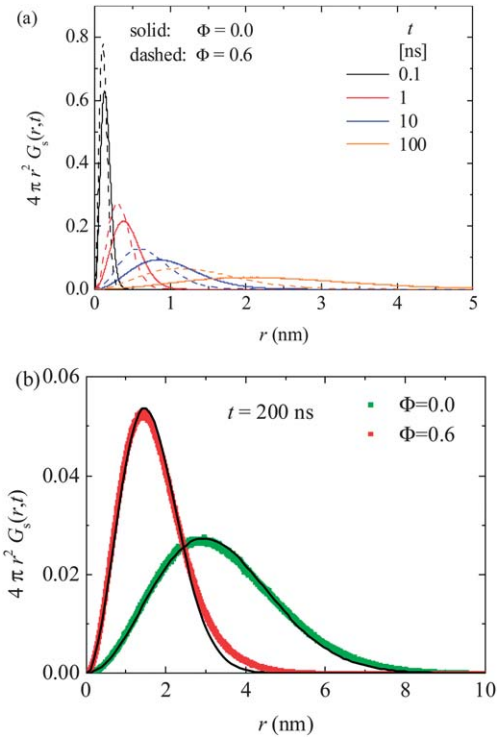

Fig. 10 Radial van Hove self-correlation functions for $\Phi = 0$ and 0.6 for (a) different times, and for (b) one selected example time to highlight the differences. The full lines are fits by a Gaussian distribution function.

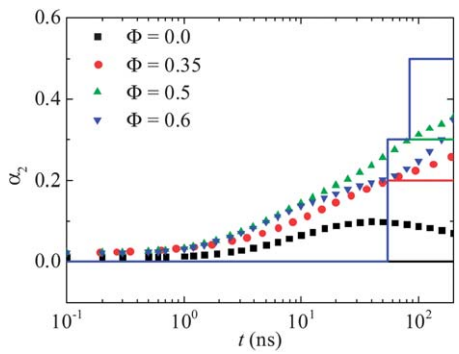

Fig. 11 Non-Gaussianity parameter α_2 for various particle fractions. The symbols are calculated from the simulations using eqn (5). The lines represent α_2 from the experimental data.

Furthermore, $\alpha_2(t)$ assumes higher values for higher particle concentrations. For comparison, we included the $\alpha_2(t)$ from the experiments. Even though, our experimental data do not allow to calculate the full time dependency, at least within the experimental accuracy similar values are obtained.

V Discussion

Before we address the diffusion behavior we want to rationalize our results of an unchanged segmental dynamics, in comparison to the simulations reported in the literature. For polymer particle interactions on the order of $\varepsilon > k_BT$ MD-simulations show a significant impact on the mode relaxation spectrum.[48] On the other hand for weak polymer particle interactions $\varepsilon < k_BT$ the work of Dionne[48] finds no change of the Rouse mode spectrum, as long as the typical chain dimensions are smaller than the nanopore sizes. From this point of view and remembering that we are dealing solely with impenetrable space, it is not surprising that the segmental relaxation of the PEP3k chains is not affected.

The main observation of this work is the reduction of chain c.m.-diffusion in the nanocomposite even at times before the geometrical confinement is explored by the moving chains. This behavior is presented in Fig. 6, where it is clear that the average distances between the polymer center of mass and the surfaces are too large to affect the chain motion directly. For our time window this conclusion remains valid, even for the samples with high silica concentrations.

To quantify this behavior further, we simulated the impact of a geometrical confinement on coarse grained polymers within the framework of the Asakura–Oosawa model. The result, as shown in Fig. 7, suggests that the contribution of geometrical confinement to the reduction of the diffusion coefficient is not significant within our time window. For the $\Phi = 0.3$ sample where an important reduction was observed it is even almost negligible. For the case of geometrical confinement alone, we conclude that for our space time frame larger effects on diffusion are not expected.

In order to understand the origin of the reduced diffusion in the nanocomposite, even at short times, we want to briefly go back to the neat melt. There, in the time window of our experiment, two different time regimes can be identified. A diffusive part well described by the Rouse diffusion for times $t > \tau_R$. For $t < \tau_R$ the neat melt shows subdiffusive motion (Fig. 5a). This short time region can be related to the motion of chains which are subject to a finite interchain interaction as described in the literature.[37,38,44–47] Even though the origin of these interactions, and therefore its physical meaning, is under discussion[44] it suggests that interchain interactions are at the origin of the subdiffusion of the center of mass motion.

To test this idea further, we performed simulations within the RaPiD model that allows taking explicitly into account such interchain interactions. Adjusting the input parameters of the model we adapted these interactions in matching the dynamics of the pure melt. We then assume that the interchain interaction between the coarse grained polymers does not change due to the addition of particles. This is justified, because the hard sphere interactions are explicitly taken into account by the algorithm.

Important is the physical soundness of the parameters obtained. The friction parameter ζ agrees well with the result of Rouse. The overlap relaxation decay length λ relates well to the radius of gyration and also the decay time for the most likely distance between neighboring chains agrees well with the Rouse time. Thus, we have found a sound description of the pure melt. As alluded to before for the filled samples no additional parameters were introduced or changed. As the fraction of colloids is increased a collective decrease of the polymer diffusion is found as in the experiments. Even at short

times $t < 100$ ns the diffusion is now influenced by an increase of Φ (see Fig. 8). These results are significantly different from the simulations within the Asakura–Oosawa model: there, an influence on the dynamics was observed only at long times when the local surroundings were sufficiently sampled by the particle. From the simulations we know that at earlier times, the interaction between the particles causes a slow-down of the polymer dynamics. In the simulations, the time-regime at which the interaction between polymers is significant is determined by the overlap relaxation time τ (see the Theory section). As colloids are added to the system the dynamics of polymers close to the interface of these colloids are directly influenced. This influence is then passed on to all other polymers that are in direct contact with the polymers at the interface. As a result, the effect of the added colloids is transported to all polymers in the system through the polymer–polymer interaction and a collective slow-down of the dynamics results even at short times (see Fig. 9 and 10).

In the above discussion we have not considered explicitly the fraction of polymers with centers of mass close to the surface. Now we want to address these polymers closer, *i.e.* the case where we expect confinement induced phenomena. In the experimental results we find clear signatures for heterogeneities in terms of the non-Gaussian behavior for $t > \tau_R$.

First we want to address the non-Gaussianity, as quantified by the parameter $\alpha_2(t)$. The experiments reveal an increase of α_2 with time and at large times with increasing particle fraction. The more detailed numerical analysis agrees semi-quantitatively with this observation. In the case of the composite the existence of heterogeneities must relate the random environment of hard spheres. However, $\alpha_2(t)$ does not allow us to address this question directly.

Therefore, we addressed this question by our simulations. We selected the fastest and slowest 10% of the polymer chains and have plotted the c.m. displacement in Fig. 12. For the pure melt we observe a spread related to the Gaussian distribution of displacements. By adding nanoparticles, the fastest chains are significantly less slowed down than the slowest polymers. Seemingly as colloids are added, polymers close to the interface are significantly slowed down. Their displacements are basically unaffected by the total amount of colloids – the slowest 10% are already strongly slowed down for $\Phi = 0.35$, but almost no change is found as Φ is increased further. The fastest polymers, however, are slowed down as Φ is increased. This agrees with the explanation that polymers close to the interface impact the dynamics of polymers in the bulk phase. With increasing Φ more polymers are affected and a general slow-down is observed.

Finally, we like to address the observed subdiffusivity at times $t > \tau_R$, for the high concentration samples ($\Phi = 0.5$, and 0.6). It is clear that this subdiffusivity phenomenon cannot be caused by the same molecular origin as the short time subdiffusive behavior that results from interchain interaction. Fig. 12 provides a tentative explanation. There we observe that the increase of $\langle r^2_{c.m.}(t)\rangle$ with time for the slowest 10% chains is significantly retarded compared to the faster chains. In addition, the slope of the increase is weaker. With increasing Φ this

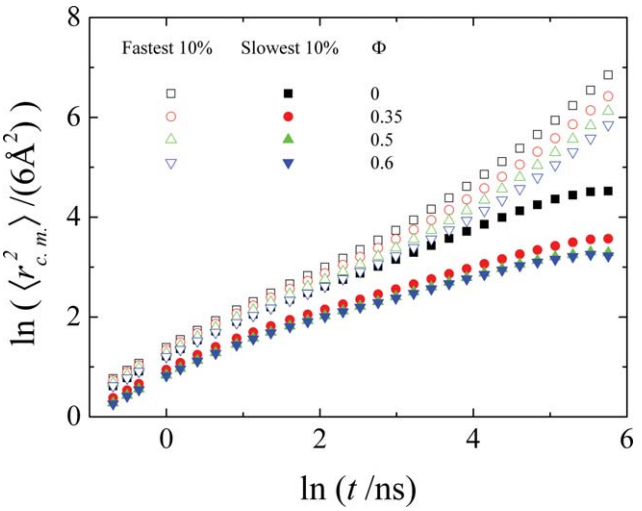

Fig. 12 Mean squared displacement of the fastest 10% and the slowest 10% of the polymers at various particle fractions.

effect must be amplified, because with increasing particle fraction the relative fraction of the slow polymers increase and therefore, the apparent subdiffusivity for $t > \tau_R$ may be related to the increasing heterogeneity due to the slow polymers. In principle there would be a direct way to proof this argument. As laid out by Moreno and Colmenero[49] the difference between intrinsic subdiffusivity and apparent subdiffusivity due to heterogeneities can be distinguished by the Q-dependence of the characteristic relaxation time. Unfortunately the quality and time range of our data do not allow this distinction.

VI Summary

We studied the polymer dynamics of a mixture of silica nanoparticles and unentangled poly(ethylene-*alt*-propylene) (PEP). The silica particle surface is coated by short hydrocarbons rendering them hydrophobic. By that means, the system becomes essentially repulsive and should avoid all adhesion effects. Our neutron spin echo experiments revealed that there is a strong deceleration of the polymer center of mass motion. But even at the highest silica fraction, the segmental chain dynamics is not affected. This coincides with recent simulations[48] that predict no change of the segmental dynamics for weak polymer particle interactions. On the other hand, we have observed an important slowing down of the center of mass diffusion already at earlier times. We noticed that the pure geometrical confinement of the Asakura–Oosawa model is not able to explain this strong influence of the colloids on the diffusion of polymer chain in the system. Only at times $t > 100$ ns does the geometrical confinement start to play a role. For times $t < 100$ ns the interaction between polymer chains causes a change of the overall diffusion coefficient in the system. Only polymers in contact with the colloids are directly affected. Due to the interchain interactions, however, also polymers in the bulk-phase which are not in direct contact with the colloids are now influenced and a collective slow-down of the dynamics results.

Appendix

All single particle simulation models for polymers, in which forces derive from some potential of mean force alone, fail to capture the effects of slow internal degrees of freedom and topological constraints. The instantaneous forces acting on the center of mass of a polymer are not just equal to the average forces determined by the configuration of the centers of mass of all other polymers, but strongly depend on information about the configuration on smaller scales, such as for example the primitive path in reptation theory. Of course, any simulation in which the polymers are represented by sufficiently long chains of connected beads will reveal these correlations and their influence on the center of mass diffusion of the chains. Such simulations, however, are prohibitive if one wants to simulate about 6000 polymers in confined geometries, for times long enough to reach the diffusive limit. In a coarse grain simulation when each polymer is represented by its center of mass, one must put in by hand the effects of slow internal motions and topological constraints. This can be done either by including memory terms into the forces in a Langevin type of simulation or by introducing a small additional set of degrees of freedom roughly describing the processes that give rise to the memory. Since with Langevin dynamics time steps become severely limited when frictions are large, the RaPiD model opts for the second approach of slightly extending the number of degrees of freedom in combination with a Brownian dynamics propagator.

We assume that the relevant small scale information can roughly be described by an additional set of dynamic variables, n_{ij}, one for each pair of polymers within a prescribed distance of $2.5R_g$ with R_g being the radius of gyration. The deviations of the n_{ij} from their equilibrium values $n_0(R_g)$ are taken to give rise to the differences between the instantaneous forces and the average forces governed by the potential of mean force. For further motivation we refer to ref. 27. Since the dynamics of polymers as a whole is largely overdamped, we use Brownian dynamics to propagate the configuration in time:

$$\frac{\mathrm{d}\vec{R}_i}{\mathrm{d}t} = -\frac{1}{\zeta_i}\frac{\partial A}{\partial \vec{R}_i} - \frac{\alpha}{\zeta_i}\left(n_{ij} - n_0\left(R_{ij}\right)\right)\frac{\partial n_0\left(R_{ij}\right)}{\partial \vec{R}_i} + \frac{\partial}{\partial \vec{R}_i}\frac{k_\mathrm{B}T}{\zeta_i} + \sqrt{\frac{2k_\mathrm{B}T}{\zeta_i \mathrm{d}t}}\vec{\Theta}$$

$$\frac{\mathrm{d}n_{ij}}{\mathrm{d}t} = -\frac{n_{ij} - n_0\left(R_{ij}\right)}{\tau_{ij}} + \sqrt{\frac{2k_\mathrm{B}T}{\alpha\tau_{ij}\mathrm{d}t}}\Theta \tag{A1}$$

here $A(R^{3N})$ is the potential of mean force, ζ_i the friction coefficient of particle i, τ_{ij} the characteristic time for the relaxation of n_{ij} towards its equilibrium value, and α a measure for the strength of the non-equilibrium forces; $\vec{\Theta}$ is a random vector with zero mean and unit variance for each of its components, while similarly Θ is a random number with zero mean and unit variance. We refer to ref. 25 for information on the potential of mean force and the equilibrium overlap functions. The friction coefficients are calculated according to

$$\zeta_i = \zeta_0 \sum_j \sqrt{n_{ij} n_0\left(R_{ij}\right)} \approx \zeta_0 \sum_j n_{ij} \tag{A2}$$

and the characteristic relaxation times of the overlap parameters as

$$\tau_{ij} = \tau_0 \exp\left(-\frac{R_{ij}}{\lambda}\right) \tag{A3}$$

The distance dependence of the characteristic relaxation times reflects the fact that slightly overlapping polymers penetrate and segregate, *i.e.* relax to equilibrium, easier than strongly overlapping polymers. It is perhaps useful to make one comment concerning the strength of the transient forces. One may easily check that the RaPiD model is invariant under the transformation $\alpha \rightarrow \alpha s^2$, $n_0 \rightarrow n_0/s$. As a result we are free to choose any normalization for n_0, which then fixes the value of α. As already mentioned, in this paper we have chosen the same normalization as in ref. 25.

The stationary distribution of the above propagator is just the Boltzmann distribution

$$P\left(R^{3N}, n^M\right) \propto \exp\left(-\left[A\left(R^{3N}\right) + \frac{\alpha}{2}\sum_{\text{pairs}}\left(n_{ij} - n_0\left(R_{ij}\right)\right)^2\right] \Big/ k_\mathrm{B}T\right) \tag{A4}$$

After integrating out the n_{ij}, for sufficiently large α, we are left with the correct distribution of the centers of mass.

To understand the importance of the approach, let us summarize in words the main ingredients and approximations of the RaPiD model. Each polymer is represented by its center of mass. Since no good separation of time scales exists, memory terms must be included in order to get the correct equations of motion of the centers of mass. The easiest way to simulate memory is by introducing a small number of additional degrees of freedom mimicking the processes responsible for the memory as much as possible. The most important process governing the dynamics of the centers of mass of polymers is the mixing and demixing of topologically constrained chains when they overlap. RaPiD introduces additional dynamical variables mimicking this process.

Acknowledgements

K.N. is grateful for the financial support by the Evonik Stiftung.

Notes and references

1 F. W. Starr, T. B. Schrøder and S. C. Glotzer, *Macromolecules*, 2002, **35**, 4481–4492.
2 H. Montes, F. Lequeux and J. Berriot, *Macromolecules*, 2003, **36**, 8107–8118.
3 J. Liu, D. Cao, L. Zhang and W. Wang, *Macromolecules*, 2009, **42**, 2831–2842.
4 I. M. Kalogeras and E. R. Neagu, *Eur. Phys. J. E*, 2004, **14**, 193–204.
5 R. B. Bogoslovov, C. M. Roland, A. R. Ellis, A. M. Randall and C. G. Robertson, *Macromolecules*, 2008, **41**, 1289–1296.
6 M. Krutyeva, J. Martin, A. Arbe, J. Colmenero, C. Mijangos, G. J. Schneider, T. Unruh, Y. Su and D. Richter, *J. Chem. Phys.*, 2009, **131**, 174901.
7 G. D. Smith, D. Bedrov, L. Li and O. Byutner, *J. Chem. Phys.*, 2002, **117**, 9478.

8 Y. Li, D. Wei, C. C. Han and Q. Liao, *J. Chem. Phys.*, 2007, **126**, 204907.
9 R. C. Picu and A. Rakshit, *J. Chem. Phys.*, 2007, **126**, 144909.
10 K. Hagita, D. Ishizuka and H. Takano, *J. Phys. Soc. Jpn.*, 2001, **70**, 2897–2902.
11 A. Milchev, *J. Phys.: Condens. Matter*, 2011, **23**, 103101.
12 J. Martín, M. Krutyeva, M. Monkenbusch, A. Arbe, J. Allgaier, A. Radulescu, P. Falus, J. Maiz, C. Mijangos, J. Colmenero and D. Richter, *Phys. Rev. Lett.*, 2010, **104**, 197801.
13 A. Baumgärtner and M. Muthukumar, *Advances in Chemical Physics*, John Wiley & Sons, Inc., chap. Polymers in Disordered Media, 1996, vol. XCIV, pp. 625–708.
14 G. I. Nixon and G. W. Slater, *Phys. Rev. E: Stat. Phys., Plasmas, Fluids, Relat. Interdiscip. Top.*, 1999, **60**, 3170–3173.
15 D. Richter, M. Monkenbusch, A. Arbe and J. Colmenero, *Adv. Polym. Sci.*, 2005, **174**, 1–221.
16 A. Arbe, J. Colmenero, B. Farago, M. Monkenbusch, U. Buchenau and D. Richter, *Chem. Phys.*, 2003, **292**, 295–309.
17 Y. Li, M. Kröger and W. K. Liu, *Phys. Rev. Lett.*, 2012, **109**, 118001.
18 J. T. Padding and W. J. Briels, *J. Chem. Phys.*, 2002, **117**, 925.
19 J. T. Kalathi, G. S. Grest and S. K. Kumar, *Phys. Rev. Lett.*, 2012, **109**, 198301.
20 N. Kikuchi and J. Horbach, *Europhys. Lett.*, 2007, **77**, 26001.
21 K. Kim, K. Miyazaki and S. Saito, *Eur. Phys. J. Spec. Top.*, 2010, **189**, 135–139.
22 F. Hoefling, T. Franosch and E. Frey, *Phys. Rev. Lett.*, 2006, **96**, 165901–165904.
23 S. Asakura and F. Oosawa, *J. Chem. Phys.*, 1954, **22**(7), 1255–1256.
24 K. Nusser, G. J. Schneider, S. Neueder, M. Meyer, W. Pyckhout-Hintzen, L. Willner, A. Radulescu and D. Richter, *Macromolecules*, 2010, **43**, 9837–9847.
25 P. Kindt and W. J. Briels, *J. Chem. Phys.*, 2007, **127**, 134901.
26 A. van den Noort, W. K. den Otter and W. J. Briels, *Europhys. Lett.*, 2007, **80**, 28003.
27 W. J. Briels, *Soft Matter*, 2009, **5**, 4401–4411.
28 I. Pagonabarraga and D. Frenkel, *J. Chem. Phys.*, 2001, **115**, 5015–5026.
29 J. T. Padding and W. J. Briels, *J. Phys.: Condens. Matter*, 2011, **23**, 233101.
30 M. Brodeck, F. Alvarez, A. Arbe, F. Juranyi, T. Unruh, O. Holderer, J. Colmenero and D. Richter, *J. Chem. Phys.*, 2009, **130**, 094908.
31 D. Richter, B. Farago, R. Butera, L. J. Fetters, J. S. Huang and B. Ewen, *Macromolecules*, 1993, **26**, 795–804.
32 G. J. Schneider, K. Nusser, L. Willner, P. Falus and D. Richter, *Macromolecules*, 2011, **44**, 5857–5860.
33 W. Paul, G. D. Smith, D. Y. Yoon, B. Farago, S. Rathgeber, A. Zirkel, L. Willner and D. Richter, *Phys. Rev. Lett.*, 1998, **80**, 2346–2349.
34 G. D. Smith, W. Paul, M. Monkenbusch and D. Richter, *Chem. Phys.*, 2000, **261**, 61–74.
35 G. D. Smith, W. Paul, M. Monkenbusch and D. Richter, *J. Chem. Phys.*, 2001, **114**, 4285–4288.
36 M. Zamponi, A. Wischnewski, M. Monkenbusch, L. Willner, D. Richter, P. Falus, B. Farago and M. G. Guenza, *J. Phys. Chem. B*, 2008, **112**, 16220–16229.
37 G. Yatsenko, E. J. Sambriski, M. A. Nemirovskaya and M. Guenza, *Phys. Rev. Lett.*, 2004, **93**, 257803.
38 E. J. Sambriski, G. Yatsenko, M. A. Nemirovskaya and M. Guenza, *J. Chem. Phys.*, 2006, **125**, 234902.
39 N. Fatkullin and R. Kimmich, *Phys. Rev. E: Stat. Phys., Plasmas, Fluids, Relat. Interdiscip. Top.*, 1995, **52**, 3273–3276.
40 T. Bickel, *Phys. A*, 2007, **377**, 24–32.
41 T. Bickel, *Phys. A*, 2007, **381**, 532, (Erratum to Ref. [Bickel2007]).
42 A. Rahman, K. S. Singwi and A. Sjölander, *Phys. Rev.*, 1962, **126**, 986–996.
43 R. Zorn, *Phys. Rev. B: Condens. Matter*, 1997, **55**(10), 6249–6259.
44 J. P. Wittmer, A. Cavallo, H. Xu, J. E. Zabel, P. Polinska, N. Schulmann, H. Meyer, J. Farago, A. Johner, S. P. Obukhov and J. Baschnagel, *J. Stat. Phys.*, 2011, **145**, 1017–1126.
45 J. Farago, A. N. Semenov, H. Meyer, J. P. Wittmer, A. Johner and J. Baschnagel, *Phys. Rev. E: Stat., Nonlinear, Soft Matter Phys.*, 2012, **85**, 051806.
46 J. Farago, H. Meyer, J. Baschnagel and A. N. Semenov, *Phys. Rev. E: Stat., Nonlinear, Soft Matter Phys.*, 2012, **85**, 051807.
47 I. S. Santos de Oliveira, A. van den Noort, J. T. Padding, W. K. den Otter and W. J. Briels, *J. Chem. Phys.*, 2011, **135**, 104902.
48 P. J. Dionne, R. Ozisik and C. R. Picu, *Macromolecules*, 2005, **38**, 9351–9358.
49 A. J. Moreno and J. Colmenero, *J. Chem. Phys.*, 2006, **125**, 164507.

